

Bachelorarbeit
zur Erlangung des akademischen Grades
Bachelor of Science

Zachary Schellin
376930

October 27, 2020

Contents

Contents	1
1 Introduction	1
1.1 State of the art	2
1.2 Objective of this thesis	2
1.3 Thesis outline	2
2 The BGK Equation	2
3 Reduced Order Algorithms	2
3.1 Data Sampling	2
3.2 POD	2
3.3 Autoencoders	3
4 Results and Latent Manifold Properties	3
4.1 Evaluation Methods	3
4.2 Results	4
4.3 Discussion and Outlook	4
References	4

1 Introduction

The Bhatnagar, Gross, Krook equation (BGK) is a kinetic collision model of ionized and neutral gases valid for rarefied as well as other pressure regimes [1]. Generating data of such a flow field is essential for various industry and scientific applications[REF]. With the intention to reduce time and cost during the data generating process, experiments were substituted with computational fluid dynamics (CFD) computations. Consequently

reduced-order models (ROMs) coupled to aforementioned computations were introduced to further the reduction of time and cost. The thriving field of artificial intelligence appears since the 80's in model order reduction for data visualization/analysis and has now surfaced in fluid mechanics. This thesis will cover the use of artificial intelligence for model order reduction in fluid mechanics.

1.1 State of the art

State of the art model reduction of dynamical systems is done via proper orthogonal decomposition (POD) which is an algorithm incorporating singular value decomposition (SVD)[3][2].

1.2 Objective of this thesis

Due to the non-linearity of transport problems in particular shock fronts, the construction of a robust ROM for those cases poses several challenges. Proper orthogonal decomposition (POD) and it's numerous variants like shifted-POD[?], POD-Galerkin[?], POD+I [?] to name only a few of them, try to solve this problem by.....

1.3 Thesis outline

2 The BGK Equation

3 Reduced Order Algorithms

3.1 Data Sampling

3.2 POD

The singular value decomposition of the input X [REF to Section 1] gives the optimal low-rank approximation \tilde{X} of X eq. (2)[Eckard-Young]. Figure 1 shows the singular values (left) and the cumulative energy (right) derived from eq. (1):

$$S_N = \sum_{k=1}^N a_k \quad \text{with a sequence} \quad \{a_k\}_{k=1}^n \quad (1)$$

$$\underset{\tilde{X}, s.t. rank(\tilde{X})=r}{\operatorname{argmin}} \quad ||X - \tilde{X}||_F = \tilde{U}\tilde{\Sigma}\tilde{V}^* \quad (2)$$

The first five singular values give an accurate approximation \tilde{X} of X . As a means to evaluate the low-rank approximation of X we will compare the density derived from eq. (5), computed from X and \tilde{X} .

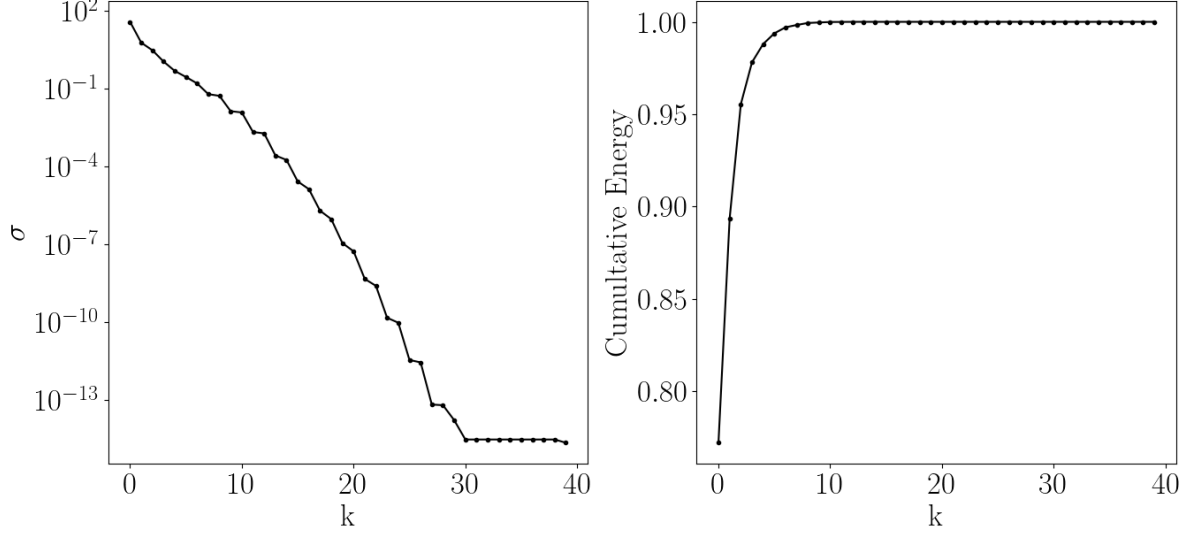


Figure 1: Singular Values (left) and cumulative energy (right) over the number of singular values

3.3 Autoencoders

The same matrix as in POD is used as input data for the autoencoder:

$$S = \begin{bmatrix} f(\xi_1, t_1, x_1) & \cdots & f(\xi_n, t_1, x_1) \\ f(\xi_1, t_1, x_2) & \cdots & f(\xi_n, t_1, x_2) \\ f(\xi_1, t_1, x_n) & \cdots & f(\xi_n, t_1, x_n) \\ f(\xi_1, t_2, x_1) & \cdots & f(\xi_n, t_2, x_1) \\ \vdots & \ddots & \vdots \\ f(\xi_1, t_n, x_n) & \cdots & f(\xi_n, t_n, x_n) \end{bmatrix}$$

During training every 1000 epochs a sample against its prediction was printed in order to link the value of the L1-Loss to a prediction. Using this method a first verification of the model was achieved. Continuing the search for any possible shortage of the models performance, that this method could not cover, eg. samples lying between every 1000 sample, that the model was not able to reconstruct correctly, a second verification process is conducted.

4 Results and Latent Manifold Properties

4.1 Evaluation Methods

In order to evaluate the proposed dimensionality reduction algorithms, two methods are being introduced. The first one constitutes a qualitative analysis using eq. (3) which measures the euclidian distance of every reconstructed sample \tilde{X}_i against its corresponding original sample X .

$$|X_i - \tilde{X}_i| = \delta_i \quad \text{with } i \text{ being the } i^{\text{th}} \text{ sample} \quad (3)$$

$$\sum |\rho_i - \tilde{\rho}_i| = \delta_\rho \quad \text{with } i \text{ being the } i^{\text{th}} \text{ sample} \quad (4)$$

As a second quantitative approach a comparison of the density over space in time of the BGK model in eq. (5) is utilized. The sum over all euclidian distances from the original samples ρ_i to their reconstruction $\tilde{\rho}_i$ is evaluated in eq. (4).

$$\int_{\mathbb{R}^3} f(\mathbf{x}, \xi, t) \begin{pmatrix} 1 \\ \xi \\ \frac{\|\xi\|^2}{2} \end{pmatrix} d\xi = \begin{pmatrix} \rho(\mathbf{x}, t) \\ \rho(\mathbf{x}, t)U(\mathbf{x}, t) \\ E(\mathbf{x}, t) \end{pmatrix} \quad (5)$$

In order to evaluate the performance of the proposed dimensionality reduction algorithms, qualitative and quantitative methods are being introduced. The qualitative analysis comprises a comparison of the sample wise test error following eq. (3) on the microscopic data. The Jacobian of the latent code is strongly linked to this measure, as it measures the contraction of the latent manifold. A quantitative measure is taken on the average test error over all over all samples of the microscopic data as well as on the macroscopic data. Both can lead to different conclusions and will be discussed in Section 4.3.

4.2 Results

A quantitative measure shows, that the linear Autoencoder performs slightly better than the POD on the input data comparing the density of the original data against the reconstruction. In contrast to this measure, the comparison of the original data to the reconstruction yields the opposite conclusion.

Algorithm	Euclidian distance in Density	Euclidian Distance	Jacobian
POD	0.151	0.0101	
AE	0.051	0.0102	
CAE 1	0.205	0.0106	
CAE 2	0.669	0.001	
CAE 2 + tw	0.385	0.0117	

4.3 Discussion and Outlook

References

- [1] Bhatnagar, Gross, and Krook. A model for collision processes in gases. 1954.
- [2] Steve L. Brunton and J. Nathan Kutz. *Data driven science and engineering*. 2019.
- [3] Thomas Franz. *Reduced-order modeling of steady transonic flows via manifold learning*. 2016.

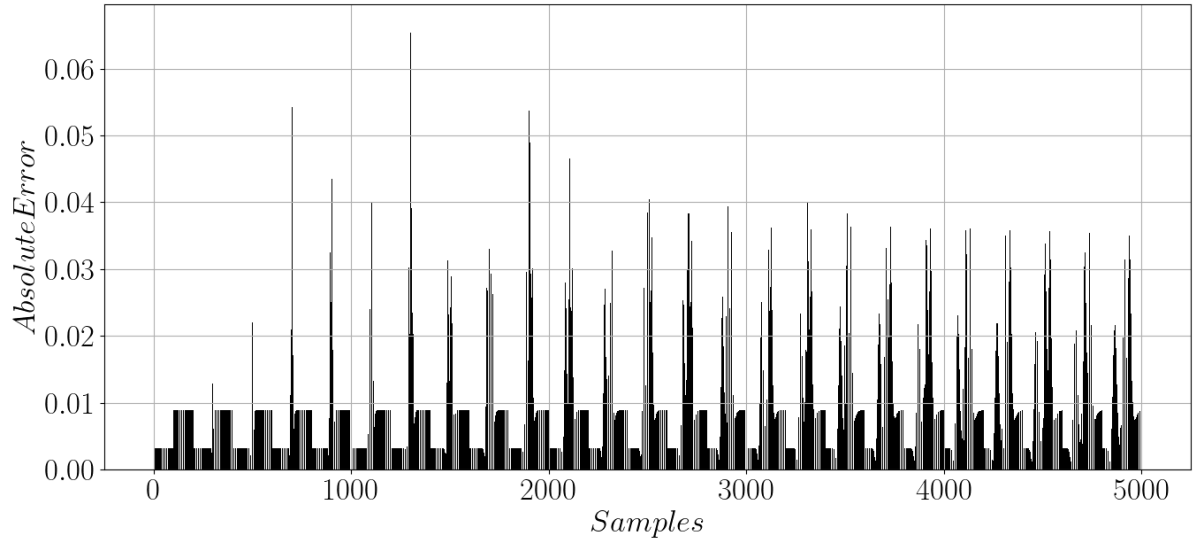


Figure 2: Absolute error for every sample in euclidean distance for the POD

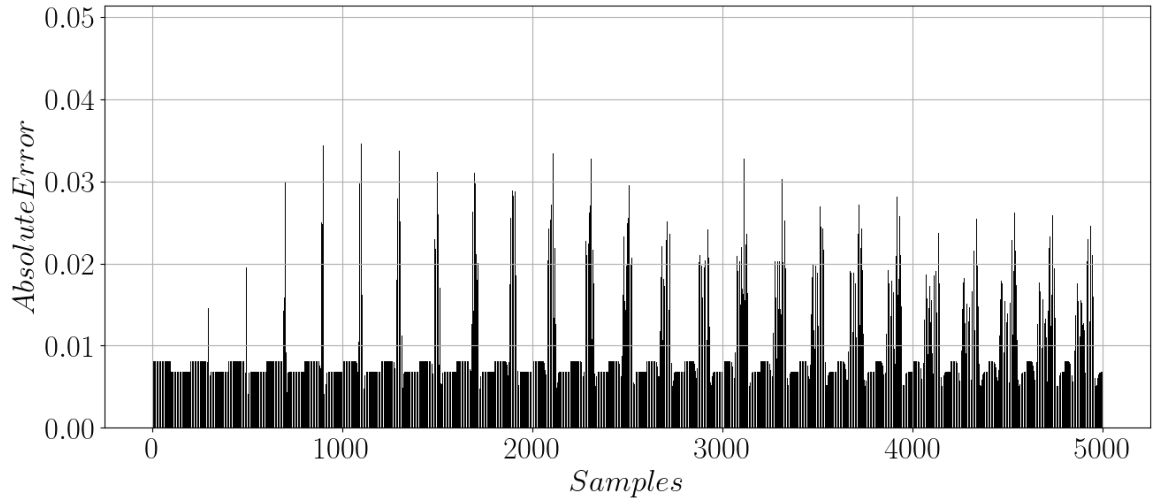


Figure 3: Absolute error for every sample in euclidean distance for the linear autoencoder

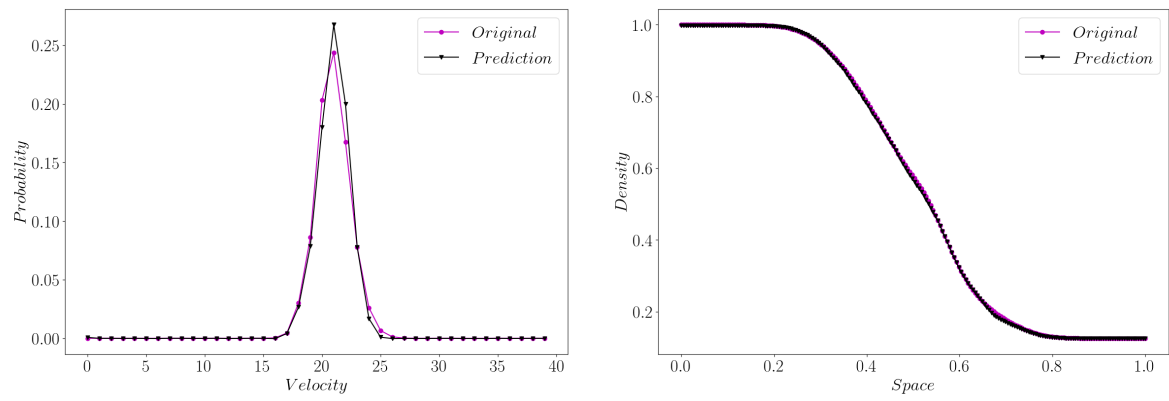


Figure 4: Error of each sample